ORIGINAL PAPER

Reconstruction of Underlying Nonlinear Deterministic Dynamics Embedded in Noisy Spike Trains

Yoshiyuki Asai · Alessandro E. P. Villa

Abstract An experimentally recorded time series formed by the exact times of occurrence of the neuronal spikes (*spike train*) is likely to be affected by observational noise that provokes events mistakenly confused with neuronal discharges, as well as missed detection of genuine neuronal discharges. The points of the spike train may also suffer a slight jitter in time due to stochastic processes in synaptic transmission and to delays in the detecting devices. This study presents a procedure aimed at filtering the embedded noise (*denoising* the spike trains) the spike trains based on the hypothesis that recurrent temporal patterns of spikes are likely to represent the robust expression of a dynamic process associated with the information carried by the spike train. The rationale of this approach is tested on simulated spike trains generated by several nonlinear deterministic dynamical systems with embedded observational noise. The application of the pattern grouping algorithm (PGA) to the noisy

Y. Asai
The Center for Advanced Medical Engineering and Informatics, Osaka University, Japan
Machikaneyama 1-3, Toyonaka, Osaka 560-8531, Japan
e-mail: asai@bpe.es.osaka-u.ac.jp

A. E. P. Villa (✉)
Grenoble Institut des Neurosciences, CR Inserm U 836-UJF-CEA-CHU,
Université Joseph Fourier, Equipe 7 - NeuroHeuristic Research Group,
UJF Site Santé - La Tronche BP 170 38042, Grenoble Cedex 9, France
e-mail: alessandro.villa@ujf-grenoble.fr

Y. Asai · A. E. P. Villa
Neuroheuristic Research Group, Information Science Institute,
HEC-University of Lausanne, Lausanne, Switzerland
URL: http://www.neuroheuristic.org/

Y. Asai
e-mail: oyasai@neuroheuristic.org

A. E. P. Villa
e-mail: avilla@neuroheuristic.org

time series allows us to extract a set of points that form the reconstructed time series. Three new indices are defined for assessment of the performance of the denoising procedure. The results show that this procedure may indeed retrieve the most relevant temporal features of the original dynamics. Moreover, we observe that additional spurious events affect the performance to a larger extent than the missing of original points. Thus, a strict criterion for the detection of spikes under experimental conditions, thus reducing the number of spurious spikes, may raise the possibility to apply PGA to detect endogenous deterministic dynamics in the spike train otherwise masked by the observational noise.

1 Introduction

A common way to study brain activity at the extracellular level consists in recording the exact times of occurrence ("epochs") of the action potentials ("spikes") generated by the nervous cell by electrophysiological means. The time series formed by the epochs of the spikes is referred to as a "spike train." A nervous cell of the brain is embedded in multiple cell assemblies and we raise the question of whether or not its spike train carries some meaningful information about the dynamics of the generative processing occurring in the neural network. Precise firing sequences (i.e., repeating intervals between epochs, with jitters of few milliseconds over a duration of several hundreds of milliseconds, that recur more often than expected by chance [1–5]) have been observed in a large set of experimental preparations and have been shown to be associated to sensorimotor and cognitive processes [6, 7]. The rationale is that recurrent spatiotemporal patterns of spikes are likely to be associated with their generative process (of whatever nature it could be). Thus, these patterns, despite their relative rarity, may represent an expression of the generative process even in the presence of observational noise.

In order to address this question, it is important to consider a kind of denoising procedure to be applied to the raw spike train and analyze to which extent it may help to recover relevant information that is associated with the activity of the recorded neuron. A pioneering study [8] gave hints about the detection of deterministic nonlinear dynamics in noisy time series by applying the pattern detection algorithm [9]. We test here the performance of the denoising effect of the pattern grouping algorithm (PGA) [10, 11] in the presence of several types and magnitudes of noise included in time series generated by the attractors of well-known dynamical systems, extending our preliminary study [12].

2 Methods

2.1 Dynamical Systems

We considered three dynamical systems well-known to exhibit chaotic behavior: two discrete mappings, i.e., the Zaslavskii map and the Ikeda map, and a continuous system of Chen equations. These dynamical systems were chosen because they embrace the range of typical chaotic behavior, but we do not consider these systems as direct models of neural dynamics.

2.1.1 Zaslavskii Map

The map [13] is defined as follows:

$$x_{n+1} = x_n + v(1 + \mu y_n) + \varepsilon v \mu \cos x_n \qquad (mod.\ 2\pi)$$

$$y_{n+1} = e^{-\gamma}(y_n + \varepsilon \cos x_n)$$

(1)

where $x, y \in \mathbf{R}$, and the parameters are real numbers with $\mu = \frac{1-e^{-\gamma}}{\gamma}$, $v = \frac{4}{3} \cdot 100$, $\gamma = 3.0$, $\varepsilon = 0.1$. The initial conditions were set to $x_0 = 0.3$ and $y_0 = 0.3$. The iterative calculation generated the time series $\{x_n\}$ that is considered for the generation of the simulated spike train.

2.1.2 Ikeda Map

The map [14] is the quadratic mapping defined as follows:

$$x_{n+1} = p + \mu(x_n \cos \theta - y_n \sin \theta)$$

$$y_{n+1} = \mu(y_n \cos \theta + x_n \sin \theta)$$

(2)

where $\theta = k - a/(1 + x_n^2 + y_n^2)$, and parameters were set to $a = 6.0$, $k = 0.4$, $p = 1.0$, and $\mu = 0.9$. Initial conditions were $x_0 = y_0 = 0.3$. The iterative calculation generated the time series $\{x_n\}$ that is considered for the generation of the simulated spike train.

2.1.3 Chen's Equation

The chaotic attractor was found [15] from the following simple system:

$$\frac{dx}{dt} = a(y - x)$$

$$\frac{dy}{dt} = (c - a)x - xz + cy$$

(3)

$$\frac{dz}{dt} = xy - bz$$

where we used $a = 35.0$, $b = 3.0$, and $c = 28.0$ as parameters and $x(0) = y(0) = 3.0$ for initial conditions. We considered a Poincaré map where the Poincaré section was defined by $\frac{dx}{dt} = 0$, and the sequence of $z(t)$ on the section was traced, referred to as $\{x_n\}$ hereinafter.

2.2 Simulated Time Series

Each of the above dynamical systems provided a time series $\{x_n\}$. A new time series $\{w_n\}$ was derived by setting $w_n = x_{n+1} - x_n + C$, where C is a constant to make all values positive, i.e., $C = -\min\{(x_{n+1} - x_n)\} + 0.1$.

The average firing frequency observed in the cerebral cortex during neurophysiological recordings is often in the range from 1 to 5 spikes/s [5, 16]. In order to generate simulated spike trains with a rate of events comparable to the neurophysiological observations, the $\{w_n\}$ were rescaled in time with a rate of 3 events/s on average. The unit time of
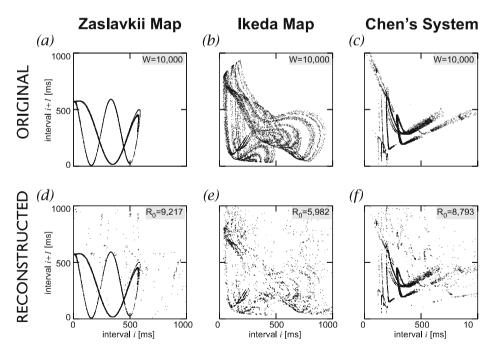
the spike trains corresponded to *milliseconds*. Each series contained ten thousand points ($N = 10,000$). The return maps, plots of w_{n+1} against w_n, of the simulated spike trains, without noise, are shown in Fig. 1a–c.

2.3 Simulated Observational Noise

We consider here two types of noise processes contributing to the observational noise in the simulated time series:

(a) An *additive noise* corresponding to the random insertion and/or deletion of points in the time series
(b) A *jitter noise* corresponding to a slight shift in time of the points in the simulated time series

The additive noise, analogous to experimental conditions, appears as spurious points in the time series, meaning the inclusion of events that were not produced by the recorded neuron, but due to external processes (e.g., the discharges of other neurons, electrical artifacts, errors in the spike sorting procedure, etc.). Another expression of the additive noise is related to those events that are associated with the generative process of the time series (i.e., the discharges of the recorded neuron) but that were missed during the experimental observation. We know from experience that this second component exists, but we can

Fig. 1 Return maps of the original plain time series W without noise (**a**–**c**) and of the time series R_0 reconstructed from the originals without noise (**d**–**f**). **a**, **d** Zaslavskii map; **b**, **e** Ikeda map; and **c**, **f** Poincaré map of Chen's dynamical system. The number of points of each reconstructed series is indicated inside each panel

only infer it without any mean of exact estimation, although its effect can be studied by using models of point processes. The jitter noise is assumed to correspond to a time shift that may appear in stochastic biological processes such as synaptic transmission and spike propagation in a neural network.

Let us assume that the original time series includes N points. The procedure to include the observational noise in the simulated time series is the following: First, deletion of $P_d\%$ of the total amount of points, chosen stochastically according to a uniform distribution, yielded a time series $\{w'\}$, which includes $N \times (1 - P_d/100)$ events. The jitter noise provoked a shift by Δt ms for each point in $\{w'\}$ yielded a time series $\{w''\}$. The value of the jitter Δt was uniformly distributed in the interval $[-J, J]$. Finally, $P_a\%$ of the total number of points were randomly added to $\{w''\}$ so as to avoid any overlap with any existing point. This overall procedure produces a noisy simulated spike train, referred to as $\{v\}$, with $N \times (1 + (P_a - P_d)/100)$ points. In this study, $N = 10,000$ and $P_d\%$ and $P_a\%$ were selected in the range $[10\%, 20\%]$.
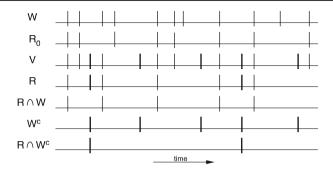
2.4 Time Series Reconstruction

Given the time series of a point process, it is possible to extract a time series formed by those points forming recurrent temporal patterns [12]. The procedure can be briefly illustrated as follows: First, the PGA detects a number of temporal patterns that repeated above the chance level in a time series, where patterns were defined as sequences composed of three or four points that were not necessarily separated by immediately successive intervals. The algorithm [10, 17] looks for all identical patterns that recurred at least n times (in this study, $n = 5$) in the time series. A clusterization procedure allows us to group those patterns whose difference in timing are lower than a threshold of accuracy (in this study, the accuracy was set to 5 ms) centered on a pattern template. A pattern template – simply referred to as "a pattern" – of a particular triplet repeating six times means that there are $3 \times 6 = 18$ points of the time series that belong to that particular triplet. Let us consider the set of points formed by all patterns detected by PGA and all repeating occurrences of those patterns. This subset of the original time series forms a time series $\{r\}$, referred to as the "reconstructed time series."

The "duration" of a particular pattern is the time interval between the first and last points of the pattern template. Only patterns with a duration shorter than a maximum interval defined by the *window duration* parameter are detected by PGA. The *jitter* parameter defines the time accuracy that is tolerated around each event forming the pattern, given the onset event. The window duration and the jitter are two parameters of the PGA algorithm that are relevant and will be discussed later in detail.

PGA was originally developed for studying spatiotemporal firing patterns in experimentally recorded spike trains [10, 17] and is applicable to any multivariate spike trains. An n-variate spike train can be considered as a projected representation of the dynamics of the observed $m(> n)$ dimensional system associated with a cell assembly in an n-th dimensional space. In the current study, for the sake of simplicity, we used only univariate spike trains as observables of neural dynamics.

2.5 Assessment of the Denoising Procedure

Let us denote the set of points in the original time series $\{w_n\}$ as W and, in the noisy time series, $\{v\}$ as V. The set of points reconstructed from the noisy time series is referred to

Fig. 2 Diagram of the time series with logical expressions. The *top line* shows a raster plot of an original time series W with *ticks* corresponding to the points in the series. The *second line* illustrates a cartoon of the time series R_0, which is a subset of W, reconstructed from the original time series. The *third line* shows a noisy time series V, generated by introducing an additive noise to the original series. *Thick ticks* in V correspond to spurious events added to W. Notice that several points of W are missing in V because they were deleted by the additive noise. For the sake of simplicity, the jitter noise is not shown here. The fourth row illustrates the reconstructed time series, denoted as R, from the noisy time series V. The *third row from the bottom*, labeled $R \cap W$, shows the points contained in the reconstructed time series from the noisy time series, as well as in the original W. This set of points is denoted as an intersection between R and W, and is shown using the notation of logical operations. The *second row from the bottom* shows W^c, which is the set of points included in the noisy time series V, but not in the original W. The *bottom line* illustrates the series formed by the points belonging to the reconstructed time series R as well as to W^c

as R (or the *denoised* time series) and the reconstructed set from the original time series (without noise) as R_0. By using logical expressions, a set of points involved in the denoised time series as well as in the original time series can be denoted as $R \cap W$. W^c represents a complementary set of W within a set $W \cup V$, i.e., a set of points either added as noise to $\{w_n\}$ or which were in $\{w_n\}$ originally but were shifted excessively with respect to the accuracy of PGA by jitter noise. The scheme of the logical relations between the above mentioned time series is illustrated in Fig. 2.

Three indices are defined to evaluate the performance of the reconstruction of time series by PGA. The first index, the *detection and reconstruction index* (DR), is defined as the ratio of the number of points in $R \cap W$ to the number of points in R_0. A larger DR means better detection of the points in the original dynamics masked by noise. The second index, which is essentially a complementary index to DR, is the *residual noise index* (RN) defined as the ratio of the number of points in $R \cap W^c$ to that in V. If the reconstruction is successful to eliminate many noisy points, then RN becomes smaller. The third index is the *effectiveness index* (EI), defined as the ratio of DR to RN, i.e., EI = DR/RN. The better the reconstruction, the larger DR and the smaller RN, yielding a larger EI.

3 Results

3.1 Reconstructed Time Series

The return maps of the reconstructed time series R_0 (without noise) for the Zaslavskii map, the Ikeda map, and the Poincaré map of Chen's equation are shown in Fig. 1d–f. The time series generated by the Zaslavskii map included 10,000 points. We found 156 groups of

patterns formed by three points (triplets) and 108 groups of quadruplets using PGA with window duration equal to 1,000 ms and with accuracy 5 ms. The overall amount of events belonging to those triplets and quadruplets was 9,217 points (i.e., 92% of the points that formed the original time series), as shown in Fig. 1d. In the case of the Ikeda map, we found 138 triplets and 148 quadruplets with the same choice of parameters for PGA, and the reconstructed time series included 5,982 points (i.e., 60% of the original series). For Chen's dynamical system, we found 174 triplets and 154 quadruplets and a reconstructed time series composed of 8,797 points (i.e., 88% of the original series). With the same conditions of noise and PGA parameters used in the present study, we observed that the reconstructed time series of the Ikeda map always contained fewer points than the series of the other dynamical systems.
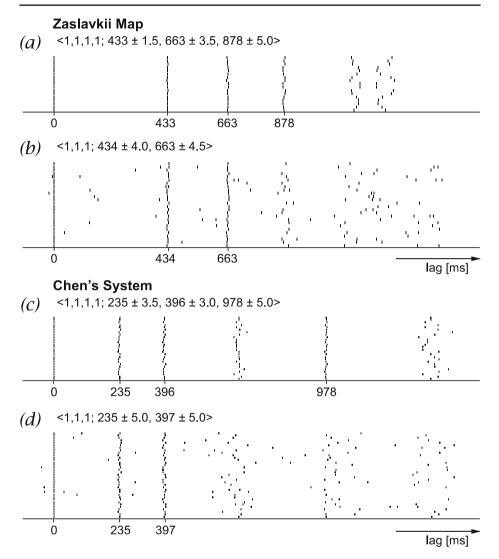
Figure 3a shows a pattern of four points found in the original time series generated by the Zaslavskii map, denoted as $< 1, 1, 1, 1; 433 \pm 1.5, 663 \pm 3.5,$ and $878 \pm 5.0 >$, where $< 1, 1, 1, 1 >$ represents the label of the events (here, we consider only univariate time series; thus, only one label set to $< 1 >$ is used here); the first event of the pattern is aligned at time 0, the second event appeared 433 ms after the first event, with a jitter ± 1.5 ms; the third and fourth events occurred 663 ± 3.5 ms and 878 ± 5.0 ms after the first event, respectively. This quadruplet recurred 17 times in the original time series W. Figure 3b shows a pattern of three points, denoted as $< 1, 1, 1; 434 \pm 4.0, 663 \pm 4.5 >$, found in the noisy time series V of the Zaslavskii map with additive noise characterized by P_d and P_a equal to 20% and with jitter noise of 5 ms. This triplet recurred 26 times and corresponded to a subset of the original quadruplet $< 1, 1, 1, 1; 433 \pm 1.5, 663 \pm 3.5, 878 \pm 5.0 >$. It is interesting to note that the fourth event of the quadruplet could not be detected due to the noise but it can be guessed when looking at the raster plot of the pattern (Fig. 3b).

An example taken from the results of Chen's dynamical system illustrates the same kind of observation. Figure 3c shows a quadruplet, denoted $< 1, 1, 1, 1; 235 \pm 3.5, 396 \pm 3.0, 978 \pm 5.0 >$, found in the original time series. Notice that a fifth-order pattern (quintuplet), with an event appearing at latency near 670 ms, could be recognized by the naked eye, but its dispersion in time was too large and was not detected by PGA under the current settings. Figure 3d shows the triplet $< 1, 1, 1; 235 \pm 5.0, 397 \pm 5.0 >$, which is a subset of the original quadruplet.
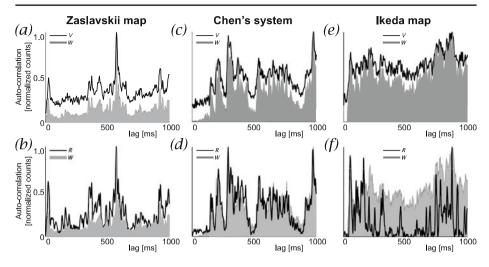
3.2 Autocorrelogram of Time Series

We calculated the autocorrelograms of W (the *original*), V (the *noisy*, with additive noise characterized by P_d and P_a equal to 20% and with jitter noise of 5 ms) and R (the *denoised reconstructed* of V) time series for all three deterministic dynamical systems (Fig. 4). Note that each autocorrelogram was normalized by its maximum peak and, in case of a Poisson point process, the curve is flat. The autocorrelograms of the W time series generated by the Zaslavskii map and Chen's system showed several sharp peaks (shaded curves in Fig. 4a–d). The noise present in the V time series tended to raise the curve baseline as shown by solid lines in Fig. 4a, c, e. In contrast, the efficiency of the denoising effect by PGA can be seen in the decrease of the baseline of the autocorrelograms (solid lines) of the R time series (Fig. 4b, d, f).

In the case of the Zaslavskii map, the baseline of the R time series almost overlapped with that of W (Fig. 4b). Notice in this figure that the peaks near 10, 400, 600, and 900 ms in the original Zaslavskii time series were well-preserved, or even enhanced, in

Fig. 3 Raster displays of spike patterns found by PGA with parameters set to window duration $= 1,000$ ms and fixed time accuracy ± 5 ms in time series of the Zaslavskii map (**a**, **b**) and in Chen's dynamical system (**c**, **d**). Patterns are aligned by their first event at time 0. **a** Quadruplets ($n = 17$) $< 1, 1, 1, 1; 433 \pm 1.5, 663 \pm 3.5, 878 \pm 5.0 >$ found in the original time series. **b** Triplets ($n = 26$) denoted as $< 1, 1, 1; 434 \pm 4.0, 663 \pm 4.5 >$ found in time series with additive noise characterized by the same amount of added and deleted points (P_d, P_a) = (20%, 20%) and with jitter noise of 5 ms. **c** Quadruplets ($n = 26$) $< 1, 1, 1, 1; 235 \pm 3.5, 396 \pm 3.0, 978 \pm 5.0 >$ found in the original time series. **d** Triplets ($n = 35$) $< 1, 1, 1; 235 \pm 5.0, 397 \pm 5.0 >$ found in the time series with the same noise used in **b**

the denoised time series. In particular, for Chen's system, the R time series showed a remarkable similarity to W (Fig. 4d) despite the fact that R contained less than half the points of the original series. The autocorrelogram of the Ikeda map was rather flat compared to the other two systems. Figure 4f shows that the baseline of Ikeda's R was much smaller than that
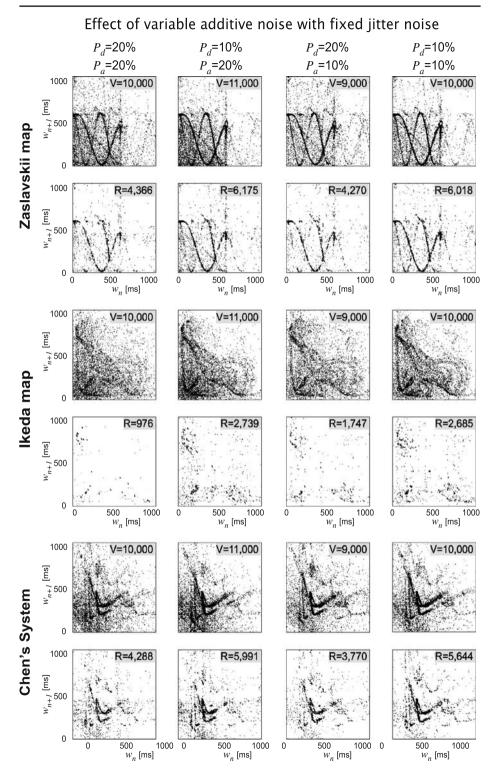
Fig. 4 The *shaded curves* in all panels show the autocorrelograms of the time series W, (i.e., the original series without noise) of the Zaslavskii map (**a**, **b**), Chen's dynamical system (**c**, **d**), and the Ikeda map (**e**, **f**). The *solid lines* in panels **a**, **c**, and **e** show the autocorrelograms of the noisy time series V, with additive noise characterized by the same amount of added and deleted points (P_d, P_a) = (20%, 20%) and with jitter noise of 5 ms. The *solid lines* in the panels **b**, **d** and **f** show the autocorrelograms of the reconstructed time series R (i.e., reconstructed from the noisy time series). All correlograms were normalized to their maximum value set to 1

of W. This effect was mainly due to the fact that the number of points in R was less than 10% of the original number of points in W. However, like the other dynamical systems, the peaks observed in Ikeda's R occurred at the same lags observed in W, often enhanced except for the broad peak near 240 ms that was finely detected but with a smaller amplitude compared to the other peaks. These results show that, despite the diversity of the dynamical systems, most of temporal features observed in the autocorrelograms of the original time series can be retrieved in the time series R, i.e., after the denoising procedure based on PGA.

3.3 Effect of Observational Noise

The denoising effect of the time series reconstruction was investigated against 12 types of noise, which were simulated as combinations of four types of additive noise, (P_d%, P_a%) = (20, 20), (10, 20), (20, 10), and (10, 10), and three levels of jitter noise, $\Delta t = 2, 5$, and 8 ms. The return maps of noisy time series V of the Zaslavskii map, the Ikeda map, and Chen's dynamical system with four types of additive noise and fixed jitter noise at 5 ms are illustrated in the upper row of panels for each system in Fig. 5. The return maps of the denoised time series R are shown in the lower row of panels. Table 1 summarizes the indices that were used to assess the performance of the denoising procedure by PGA under the presence of various types of noise.

First, we analyze the effect of *jitter noise*. For all types of additive noise and for all dynamics, the values of the DR decreased monotonously as the level of jitter noise Δt increased. Conversely, the values of the RN were minimal for $\Delta t = 5$ ms. It is interesting to notice that, with $\Delta t = 8$ ms, the level of jitter noise was larger than the accuracy used

Effect of variable additive noise with fixed jitter noise

Fig. 5 Return maps of the noisy time series V (with variable additive noise and fixed jitter noise of 5 ms) and R (reconstructed from those noisy time series) of the Zaslavskii map (*top rows*), the Ikeda map (*central rows*), and Chen's dynamical system (*bottom rows*). The parameters of PGA were set to window duration = 1,000 ms and time precision ±5 ms. Four levels of additive noise were analyzed. For each row of panels, the return maps displayed from the *left* to the *right column* of the figure refer to noise levels characterized by $(P_d, P_a) = (20\%, 20\%), (10\%, 20\%), (20\%, 10\%)$, and $(10\%, 10\%)$, where P_d and P_a correspond to the percentage of deleted and added points, respectively. The number of points of each reconstructed series is indicated inside each panel

here (±5 ms) for PGA. At such a high level of jitter noise, the value of RN increased significantly because the denoised time series still included many spurious spikes and the EI became small because of large RN and small DR values. Notice that, for a given type of noise, the values of EIs were similar for $\Delta t = 2$ and 5 ms.
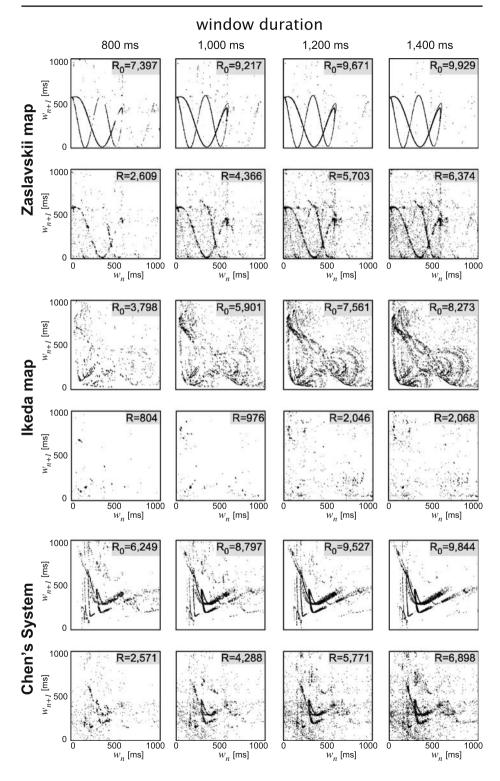
Let us compare the performance indices given the same jitter noise level within each dynamics as a function of P_d and P_a (i.e., the percentages of points deleted and added as additive noise, respectively). The values of DRs for $P_d = 20\%$ were similar, regardless of the percentage of added points, and were lower than the DR values at $P_d = 10\%$ for all dynamical systems. For example, in Chen's dynamical system with jitter noise equal to 5 ms, $DR_{(P_d=20\%, P_a=20\%)} = 41.3$ and $DR_{(P_d=20\%, P_a=10\%)} = 40.3$. With the same parameters of PGA used for pattern detection, we observed $DR_{(P_d=10\%, P_a=20\%)} = 60.9$ and $DR_{(P_d=10\%, P_a=10\%)} = 60.8$. Conversely, the values of index RN showed a tendency different from that of index DR. The RN index was maximal at noise level ($P_d = 10\%, P_a = 20\%$). Notice that the value of RN did not tend to be affected by a change in the relative number of deleted points (P_d). Conversely, the smaller the ratio of spurious added points (P_a), the smaller the index RN.

In the case of Chen's system with $\Delta t = 5$ ms, we observed RN = 4.7 and RN = 5.8 for $P_a = 20\%$ and $P_d = \{20, 10\}\%$, respectively. The values of RN (2.5 and 3.0) were lower

Table 1 Performance of the denoising procedure with different kinds of observational noise by PGA with parameters set to window duration = 1,000 ms and time precision ±5 ms

Noise		Zaslavskii map			Ikeda map			Chen's System		
P_d, P_a	Δt	DR	RN	EI	DR	RN	EI	DR	RN	EI
20%, 20%	2	56.7	5.7	10.0	27.6	2.4	11.4	53.1	5.2	10.2
	5	42.5	4.2	10.0	14.9	1.4	10.4	41.3	4.7	8.8
	8	24.3	16.1	1.5	8.9	4.4	2.0	26.1	16.3	1.6
10%, 20%	2	75.4	7.0	10.8	55.5	4.0	13.9	74.3	7.0	10.6
	5	59.9	5.3	11.3	39.4	3.5	11.3	60.9	5.8	10.5
	8	34.3	18.6	1.8	19.7	8.5	2.3	39.2	22.2	1.8
20%, 10%	2	59.2	3.4	17.2	36.5	2.1	17.6	51.3	3.0	17.2
	5	43.5	2.4	18.5	26.9	1.5	18.0	40.3	2.5	16.3
	8	22.3	13.7	1.6	11.5	5.6	2.0	25.8	15.4	1.7
10%, 10%	2	75.2	3.7	20.5	57.7	2.7	21.7	73.1	3.3	22.4
	5	61.2	3.0	20.2	41.6	2.0	21.2	60.8	3.0	20.3
	8	30.5	17.5	1.7	17.3	6.9	2.5	36.4	19.3	1.9

P_d and P_a represent the percentage of points that were deleted and added as additive noise, respectively. Δt represents the level of jitter noise as maximum time shift in [ms]

window duration

◀ **Fig. 6** Return maps of the time series R_0 (reconstructed from the original time series without noise) and R (reconstructed from the time series with additive noise characterized by P_d and P_a equal to 20% and with jitters noise of 5 ms) of the Zaslavskii map (*top rows*), the Ikeda map (*central rows*), and Chen's dynamical system (*bottom rows*). Four values of the *window duration* parameter of PGA, 800, 1,000, 1,200, and 1,400 ms, were used for detecting the significant temporal patterns. The return maps of the *leftmost column panels* refer to $w = 800$ ms, and the return maps of the *rightmost column panels* refer to $w = 1,400$ ms. Time precision of PGA was fixed at ± 5 ms. The number of points of each reconstructed series is indicated inside each panel

when P_a was reduced to 10% with either P_d. Thus, the best effectiveness (EI) was observed for the time series with additive noise characterized by $P_d = 10\%$ and $P_a = 10\%$. The second best EI was observed for $P_d = 20\%$ and $P_a = 10\%$. For the cases with $P_a = 20\%$, EI tended to decrease. Notice that, in relative terms, the difference in EI due to a change in P_d was smaller than the difference due to a change in P_a.

3.4 Effect of Window Duration

We tested window durations of 800, 900, 1000, 1200 and 1400 *ms* for PGA reconstruction of the dynamical systems. The time accuracy of PGA was fixed at ± 5 *ms*. In all cases that were analyzed, with and without noise, the number of events of the reconstructed time series was likely to increase as window duration increased, as noted elsewhere [10, 11]. For each dynamical system, Fig. 6 shows two rows of panels: in the upper row, the return maps of the time series R_0 (i.e., reconstructed from the original series without noise), and in the lower row, the return maps of the denoised time series R reconstructed from time series with additive noise $P_d = P_a = 20\%$ and jitter noise of $\Delta t = 5$ ms. The number of events included in each series is indicated inside each panel.

The performance of time series reconstruction by PGA is summarized in Table 2. Both DR and RN tended to increase as window duration increased. This means that a wider window duration might be used to retrieve more spikes included in the original time series. However, the wider the window duration, the higher the number of noisy spikes that were detected, as well. This tendency was better observed for window durations above 1,000 ms, as illustrated by a decrease of the EI.

Table 2 Performance of the denoising procedure applied to fixed observational noise with balanced additional noise ($P_d = 20\%$, $P_a = 20\%$) and jitter noise of 5 ms as a function of the PGA parameter window duration with fixed time precision of ± 5 ms

Window	Zaslavskii map			Ikeda map			Chen's system		
[ms]	DR	RN	EI	DR	RN	EI	DR	RN	EI
800	31.8	2.6	12.5	13.3	1.4	9.6	36.0	3.2	11.3
900	38.0	3.3	11.6	20.9	2.1	10.2	35.6	3.0	12.0
1,000	42.5	4.2	10.0	14.9	1.4	10.4	41.3	4.7	8.8
1,200	52.2	6.6	8.0	23.3	2.8	8.3	53.1	7.1	7.5
1,400	56.7	7.4	7.6	21.5	2.9	7.5	60.8	9.1	6.7

4 Discussion

The main assumption tested in the present study is that recurrent temporal patterns of points represent a common characteristic of the time series generated by deterministic nonlinear dynamical systems. The original dynamics may be masked in the presence of observational noise and we assume that detecting and identifying temporal patterns of points may help to reconstruct the underlying dynamics. We consider that spike trains could be good candidates for noisy time series that mask deterministic dynamics [18–22]. Our assumption was tested with simulated time series generated by known deterministic chaotic systems (i.e., the Zaslavskii map, the Ikeda map, and Chen's dynamical system) that were rescaled to spike trains whose average frequency was set to 3 spikes/s. We emphasize that these nonlinear systems are far from the system that might be generated by the cell assembly dynamics where each neuron is assumed to behave as a nonlinear dynamical system, which receives synaptic inputs and generates spikes according to its dynamics [23]. We are currently exploring the dynamics based on single neuron dynamical systems [24], but the collective dynamics that emerge from such studies is itself a matter of investigation and it could not be taken here as granted that it is a known chaotic system with a testable description.

The performance of the denoising effect obtained applying the PGA algorithm [10, 11] was tested with 12 types of simulated observational noise (provided as combinations of four kinds of additive noise and three kinds of jitter noise) superimposed on the time series. The current results confirm and extend our previous observations [8, 12]. A novel performance index defined in this study, the EI, accounts for the number of points belonging to the underlying dynamical system that are retrieved by our procedure and for the spurious points that appear in the reconstructed time series as well. It is worth reporting that the control parameters of PGA play an important role for the performance of the denoising procedure and should be considered carefully for a fair assessment. The longer the window duration (i.e., the maximum allowed duration of temporal patterns), the better the detection of points belonging to the original dynamical system time series, but the number of spurious points due to the added noise also tended to increase in the reconstructed time series. A *window duration* equal to 900 ms was a good compromise for the time series examined in this study. The value 900 ms is likely to be determined by the average firing frequency (3 spikes/s, i.e., three events in 1,000 ms), and further investigation should be carried out with other firing frequencies in order to assess more precisely the effect of all control parameters of PGA. A fair comparison with other methods aimed at filtering chaotic time series is difficult because the main methods assume the presence of a deterministic dynamics and are aimed to reduce the noise for a better study of attractor dimension or estimation of Lyapunov exponents [25]. A bad choice of parameters could lead to a significant bias in the performance of the selected method, and we prefer to offer our method to criticism and testing on benchmark data agreed by the scientific community. In the present case, we apply the PGA algorithm a priori without any condition on the underlying dynamics, and we study here its application to selected dynamical systems with noise.

We considered an observational noise due to the deletion and addition of spikes combined with a jitter noise (shift of spikes in time) as an independent process masking the intrinsic deterministic dynamics. Such noise is aimed to mimic a common problem that occurs in the extracellular electrophysiological recording of neuronal activity. The recording procedure detects the neuronal discharges (spikes) from the bioelectric signal, which is a combination of the varying electric fields detected at the electrode tip and a background noise. The first step of any recording procedure consists of setting a threshold of detection:

the lower the threshold, the higher the chance to avoid missing neuronal discharges, but also the higher the chance to detect spurious signals. The spike detection is improved by a template-matching procedure [26, 27] where certain waveforms that satisfy a criterion based on the shape of the signal are labeled as spikes. However, some stochastic fluctuations that meet the criterion may be counted as spikes. A stricter criterion would decrease the number of spurious spikes, but it would increase the risk to miss real neuronal spikes. The number of missed and spurious spikes can be compared to some extent with the observational noise that consisted in deletion and addition of spikes (P_d and P_a, respectively) simulated in this study. The decrease in the ratio of spurious spikes (P_a) improved the relative performance of the denoising procedure, in terms of the EI, more than a decrease in the ratio of deleted spikes (P_a). This tendency was consistent in all three dynamical systems examined in this study. It suggests that a strict criterion for the detection of spikes, thus reducing the number of spurious spikes, may raise the possibility to apply PGA to detect endogenous deterministic dynamics in the spike train otherwise masked by the observational noise.

Techniques developed in the field of dynamical systems offer powerful tools to explore the nature of dynamics in the observed spike trains [28]. Indices such as correlation dimension, entropy, and Lyapunov exponents can be calculated with efficient numerical methods and applied to the observed spike trains to assess the deterministic nature of the underlying process. These methods are not robust in the presence of observational noise that can impair the detection of a deterministic dynamics. The present study suggests that detection of temporal patterns of spikes may be used as a preprocessor for filtering out part of the noise and building reconstructed time series that may be more likely to retain the underlying deterministic processes, if any. This may open another way to the detection of dynamical systems in neural activity.

References

1. Dayhoff, J.E., Gerstein, G.L.: Favored patterns in spike trains. I. Detection. J. Neurophysiol. **49**, 1334–1348 (1983)
2. Abeles, M., Gerstein, G.: Detecting spatiotemporal firing patterns among simultaneously recorded single neurons. J. Neurophysiol. **60**, 909–924 (1988)
3. Villa, A.E.P., Abeles, M.: Evidence for spatiotemporal firing patterns within the auditory thalamus of the cat. Brain Res. **509**, 325–327 (1990)
4. Prut, Y., Vaadia, E., Bergman, H., Haalman, I., Slovin, H., Abeles, M.: Spatiotemporal structure of cortical activity—properties and behavioral relevance. J. Neurophysiol. **79**, 2857–2874 (1998)
5. Tetko, I.V., Villa, A.E.P.: A pattern grouping algorithm for analysis of spatiotemporal patterns in neuronal spike trains. 2. Application to simultaneous single unit recordings. J. Neurosci. Methods **105**, 15–24 (2001)
6. Villa, A.E.P., Tetko, I.V., Hyland, B., Najem, A.: Spatiotemporal activity patterns of rat cortical neurons predict responses in a conditioned task. Proc. Natl. Acad. Sci. U. S. A. **96**, 1006–1011 (1999)
7. Villa, A.E.P.: Spatio-temporal patterns of spike occurrences in freely-moving rats associated to perception of human vowels. In: König, R., Heil, P., Budinger, E., Scheich, H. (eds.) Auditory Cortex: [T]owards a Synthesis of Human and Animal Research, chap. 17, pp. 241–254. Lawrence Erlbaum, Oxford (2005)
8. Tetko, I.V., Villa, A.E.P.: A comparative study of pattern detection algorithm and dynamical system approach using simulated spike trains. Lect. Notes Comput. Sci. **1327**, 37–42 (1997)
9. Tetko, I.V., Villa, A.E.P.: Fast combinatorial methods to estimate the probability of complex temporal patterns of spikes. Biol. Cybern. **76**, 397–407 (1997)

10. Tetko, I.V., Villa, A.E.P.: A pattern grouping algorithm for analysis of spatiotemporal patterns in neuronal spike trains. 1. Detection of repeated patterns. J. Neurosci. Methods **105**, 1–14 (2001)
11. Abeles, M., Gat, I.: Detecting precise firing sequences in experimental data. J. Neurosci. Methods **107**, 141–154 (2001)
12. Asai, Y., Yokoi, T., Villa, A.E.P.: Detection of a dynamical system attractor from spike train analysis. Lect. Notes Comput. Sci. **4131**, 623–631 (2006)
13. Zaslavskii, G.M.: The simplest case of a strange attractor. Phys. Lett. **69A**, 145–147 (1978)
14. Ikeda, K.: Multiple-valued stationary state and its instability of the transmitted light by a ring cavity system. Opt. Commun. **30**, 257–261 (1979)
15. Chen, G., Ueta, T.: Yet another chaotic attractor. Int. J. Bifurc. Chaos **9**, 1465–1466 (1999)
16. Abeles, M.: Local Cortical Circuits. Springer, Heidelberg (1982)
17. Villa, A.E.P., Tetko, I.V.: Spatiotemporal activity patterns detected from single cell measurements from behaving animals. Proc. SPIE **3728**, 20–34 (1999)
18. Rapp, P.E.: Chaos in the neurosciences: cautionary tales from the frontier. Biologist **40**, 89–94 (1993)
19. Celletti, A., Villa, A.E.P.: Determination of chaotic attractors in the rat brain. J. Stat. Phys. **84**, 1379–1385 (1996)
20. Celletti, A., Villa, A.E.P.: Low dimensional chaotic attractors in the rat brain. Biol. Cybern. **74**, 387–394 (1996)
21. Celletti, A., Bajo Lorenzana, V.M., Villa, A.E.P.: Correlation dimension for two experimental time series. J. Stat. Phys. **89**, 877–884 (1997)
22. Celletti, A., Froeschlé, C., Tetko, I.V., Villa, A.E.P.: Deterministic behaviour of short time series. Meccanica **34**, 145–152 (1999)
23. Izhikevich, E.M.: Neural excitability, spiking and bursting. Int. J. Bifurc. Chaos **10**, 1170–1266 (2000)
24. Asai, Y., Yokoi, T., Villa, A.E.P.: Deterministic nonlinear spike train filtered by spiking neuron model. Lect. Notes Comput. Sci. **4668**, 924–933 (2007)
25. Kostelich, E.J., Schreiber, T.: Noise reduction in chaotic time-series data: a survey of common methods. Phys. Rev. E **48**, 1752–1763 (1993)
26. Aksenova, T.I., Chibirova, O., Dryga, A.O., Tetko, I.V., Benabid, A., Villa, A.E.P.: An un-supervised automatic method for sorting neuronal spike waveforms in awake and freely moving animal. Methods **30**, 178–187 (2003)
27. Asai, Y., Aksenova, T.I., Villa, A.E.P.: On-line real-time oriented application for neuronal spike sorting with unsupervised learning. Lect. Notes Comput. Sci. **3696**, 109–114 (2005)
28. Segundo, J.P.: Nonlinear dynamics of point process systems and data. Int. J. Bifurc. Chaos **13**, 2035–2116 (2003)